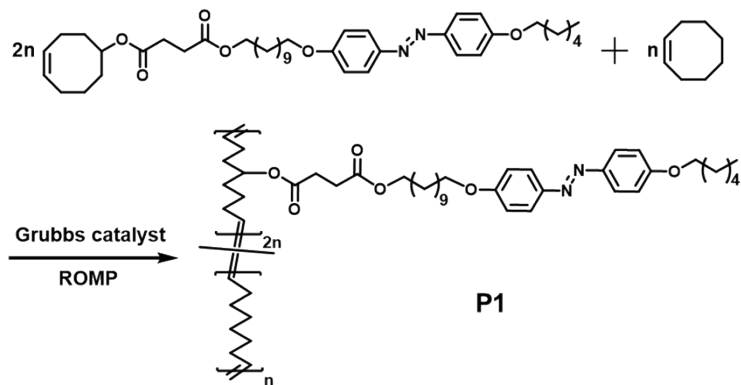


Electronic Supplementary Information

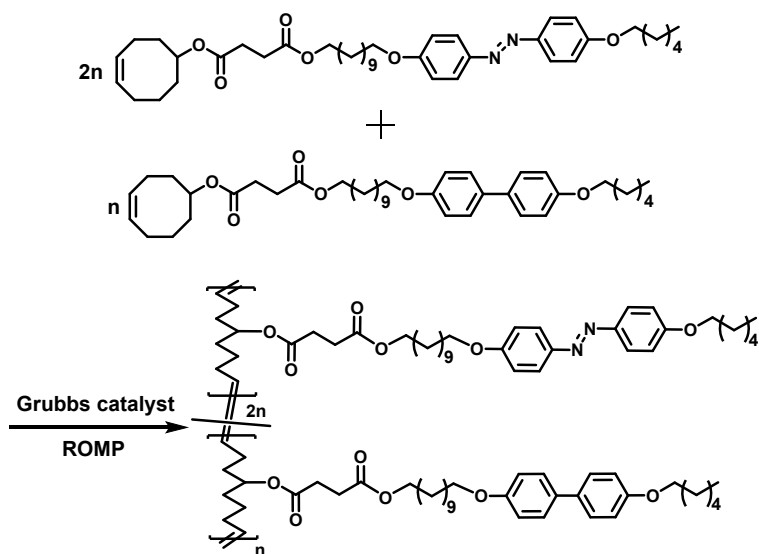
Yaoqing Feng, Jia Wei, Lang Qin* and Yanlei Yu*

*Department of Materials Science, State Key Laboratory of Molecular Engineering of
Polymers, Fudan University, 220 Handan Road, Shanghai, 200433, China.*

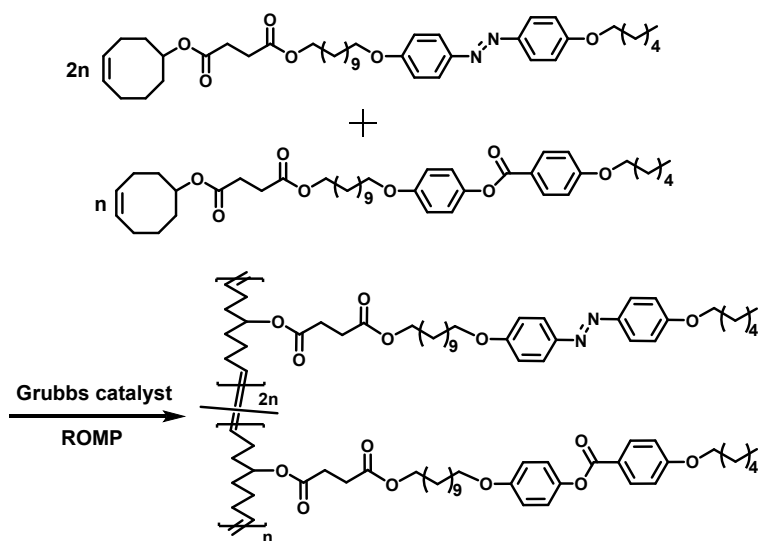
E-mail: ylyu@fudan.edu.cn ; qinlang@fudan.edu.cn



Scheme S1. Synthetic route of liquid crystal polymer P1.



Scheme S2. Synthetic route of liquid crystal polymer P2.



Scheme S3. Synthetic route of liquid crystal polymer P3.

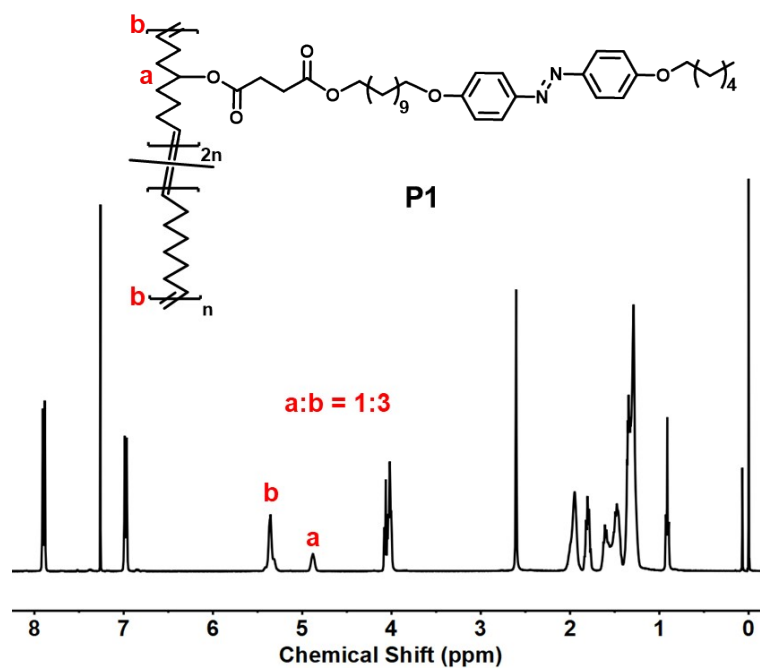


Fig. S1. The ^1H NMR spectra of P1 in CDCl_3 . The integration ratio of the peak area of a and b is about 1:3, indicating that the relative ratio of the two monomers (azobenzene monomer/cyclooctene monomer) conformed to 2:1.

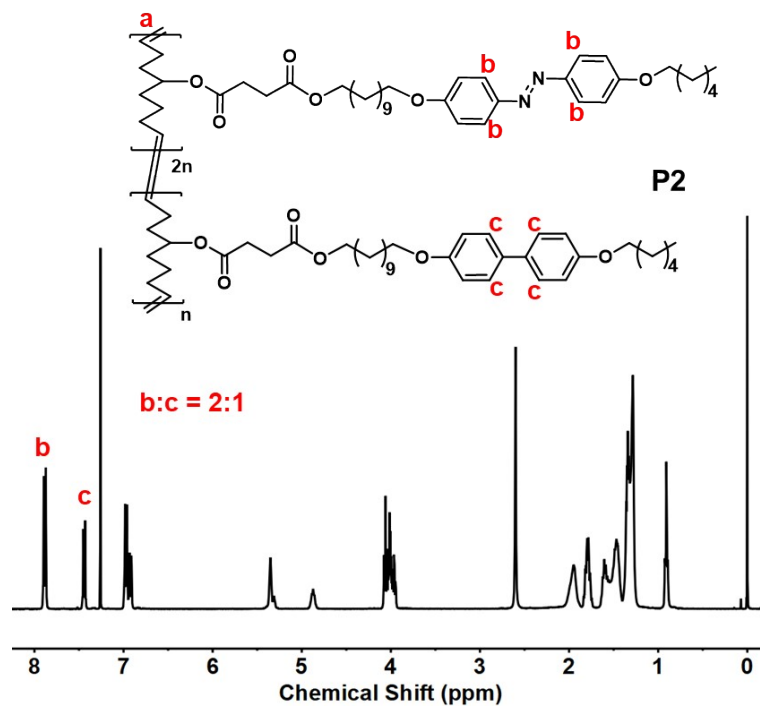


Fig. S2. The ^1H NMR spectra of P2 in CDCl_3 . The integration ratio of the peak area of b and c is about 2:1, indicating that the relative ratio of the two monomers (azobenzene monomer/biphenyl monomer) conformed to 2:1.

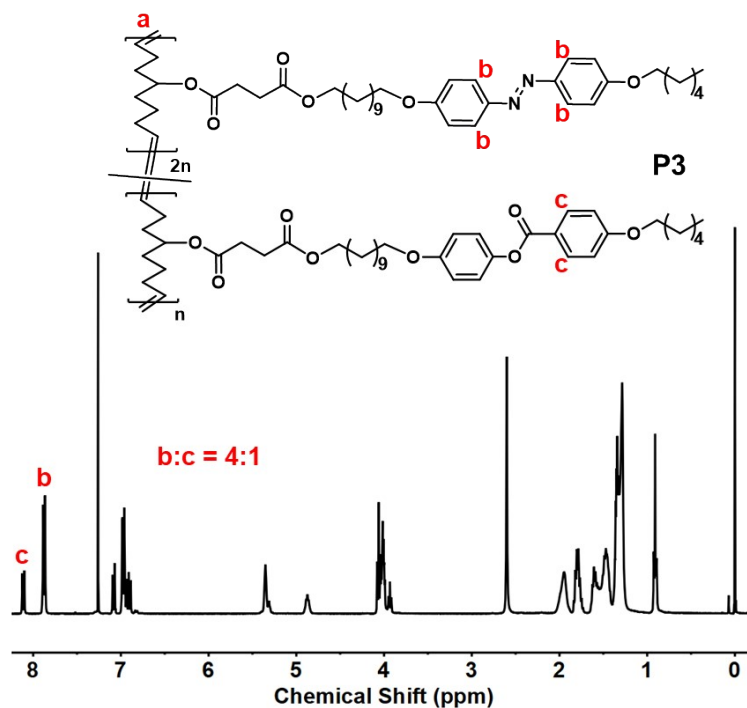


Fig. S3. The ^1H NMR spectra of P3 in CDCl_3 . The integration ratio of the peak area of b and c is about 4:1, indicating that the relative ratio of the two monomers (azobenzene monomer/phenyl benzoate monomer) conformed to 2:1.

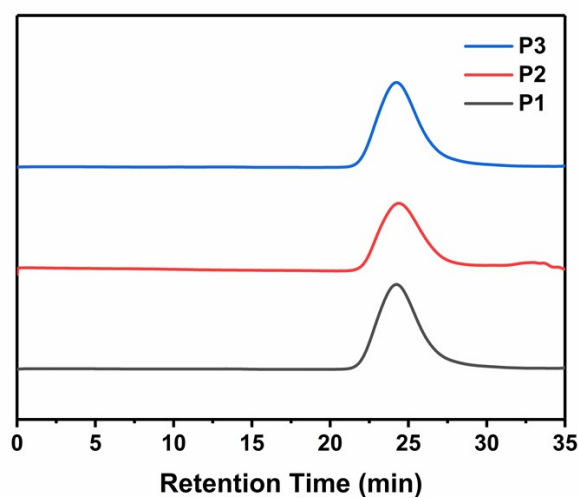


Fig. S4 The GPC curves of P1, P2, and P3.

Table S1. Characterization of the synthesized polymers.

Polymers	Monomer Feed (mmol)	Azo unit in polymer chain (mol%)	M_n (g mol^{-1})	PDI (M_w/M_n)
P1	CAB(2) COE(1.2)	64(67)	2.2×10^5	1.71
P2	CAB(2) CBP(1)	66(67)	1.9×10^5	1.74
P3	CAB(2) CBZ(1)	67(67)	2.0×10^5	1.60

^[a] The azo unit content determined by ^1H NMR spectroscopy.

^[b] The monomer feed of the azo unit.

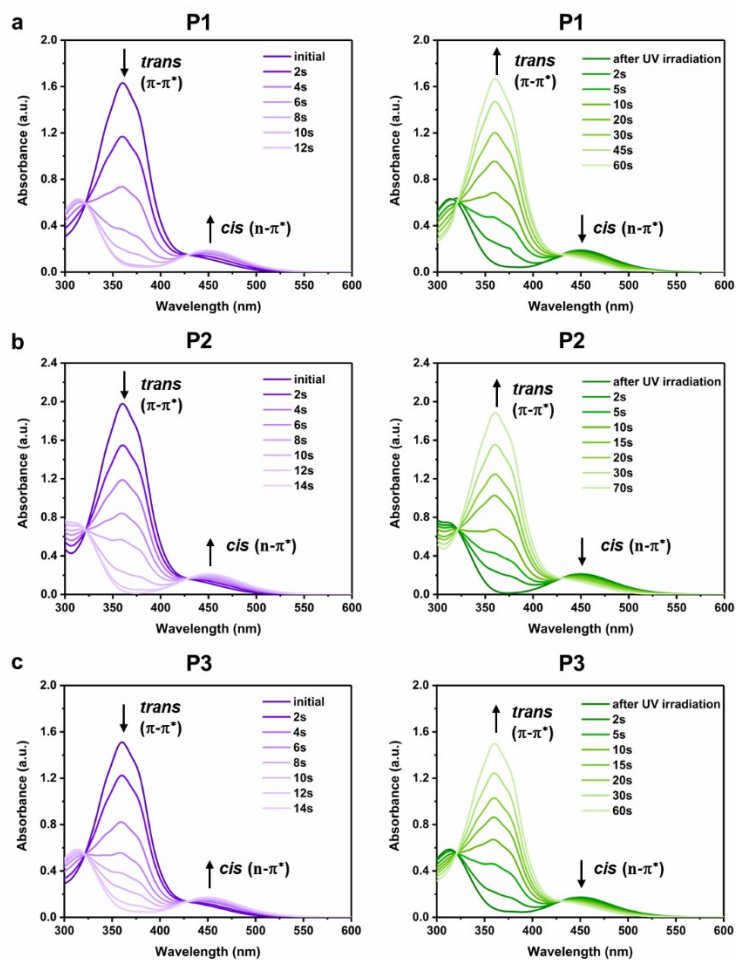


Fig.S5 Variation of the UV-vis spectra of P1, P2, and P3 induced by the UV and visible light irradiation. (a) P1 dissolved in CH_2Cl_2 solution ($c = 5 \times 10^{-4} \text{ M}$); (b) P2 dissolved in CH_2Cl_2 solution ($c = 5 \times 10^{-4} \text{ M}$); (c) P3 dissolved in CH_2Cl_2 solution ($c = 5 \times 10^{-4} \text{ M}$). UV light: 365 nm, 20 mW cm^{-2} . Visible light: 530 nm, 20 mW cm^{-2} . The isomerization degrees at the photostationary state are 96.5% (P1), 99.0% (P2), and 96.0% (P3) respectively, which are estimated from
$$\text{isomerization degree} = \frac{A_{\text{origin}} - A_s}{A_{\text{origin}}} \times 100\%$$
, where A_{origin} is the absorbance at λ_{max} before the light irradiation and A_s is the absorbance at the same wavelength measured at the photostationary state (*Macromolecules* 2006, 39, 6590-6598).

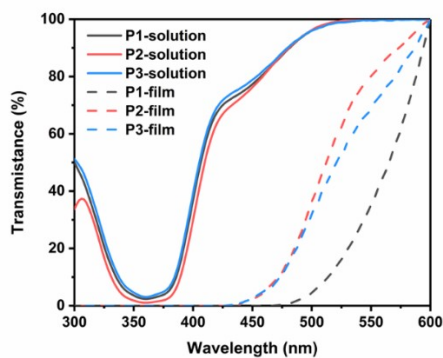


Fig.S6 The plot of the transmittance of the LCPs in film states or solution states.

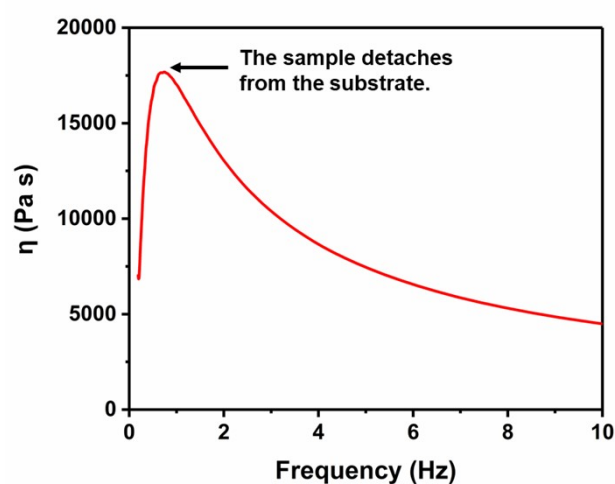


Fig. S7 The dynamic viscosity of *cis* P1. The sample separates from the substrate when the viscosity reaches its maximum value. Then the viscosity value shows a significant decrease with the increase of the rotational speed, which results from that the sample detached from the substrate rather than the shear-thinning property of the fluid.

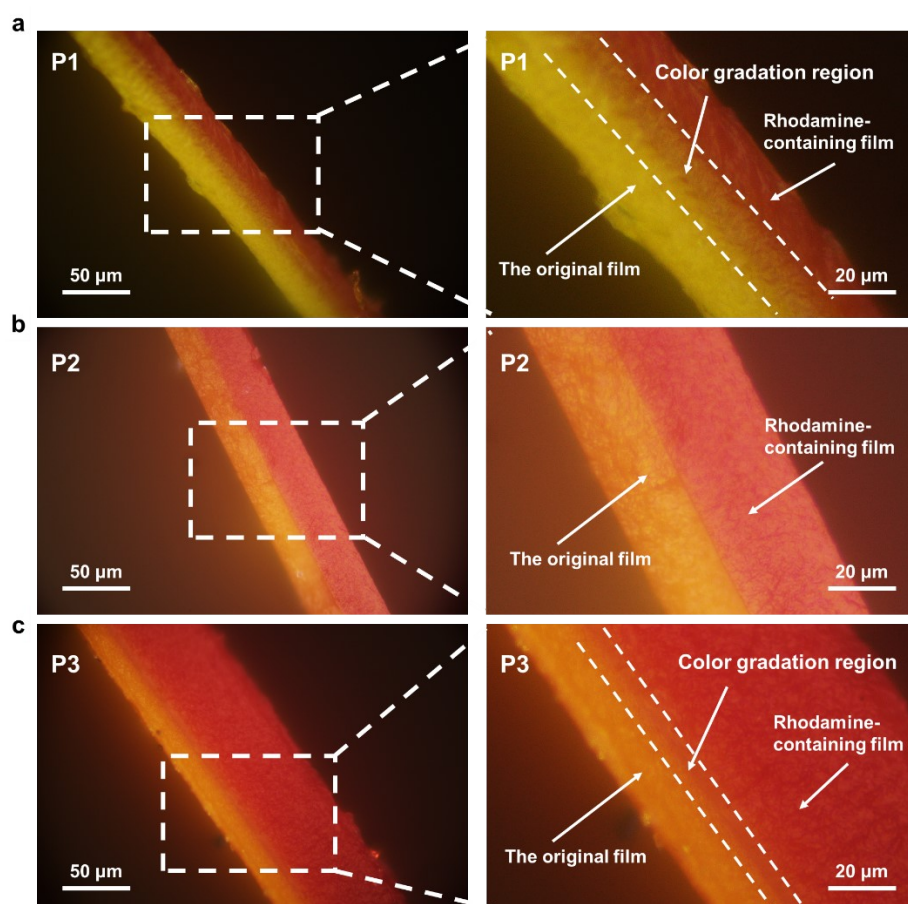


Fig. S8 Microscope images of (a) the photo-welded bilayer P1 film with a color gradation region in the center of the film; (b) the photo-welded bilayer P2 film with a clear interface in the center; (c) the photo-welded bilayer P3 film with a smaller color gradation region in the center of the film. All the rhodamine containing films (the red side) and the original films (yellow side) were fabricated by the drop-casting method.

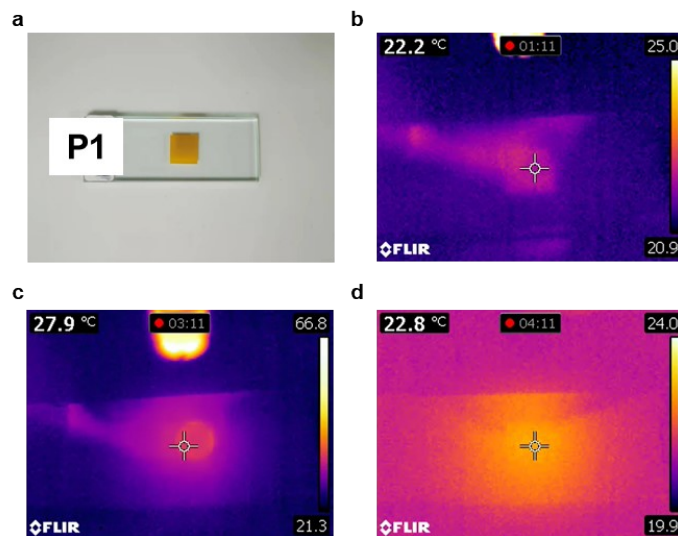


Fig. S9 The infrared thermography photographs of P1 film (b) before UV irradiation (100 mW cm^{-2}), (c) under UV irradiation for 2 min, (d) after turning off UV light for 1 min.

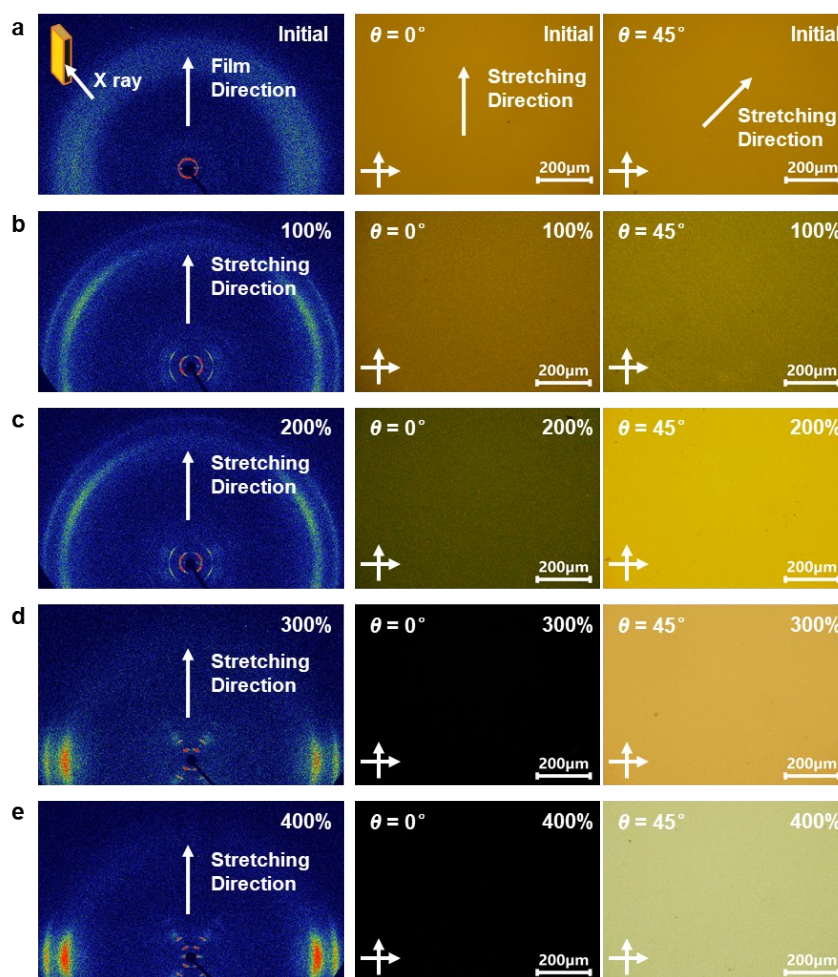


Fig. S10 2D-WAXD patterns and POM images of stretched P1 films with different stretching ratio. θ Indicates the angle between the polarizer and the stretching direction.

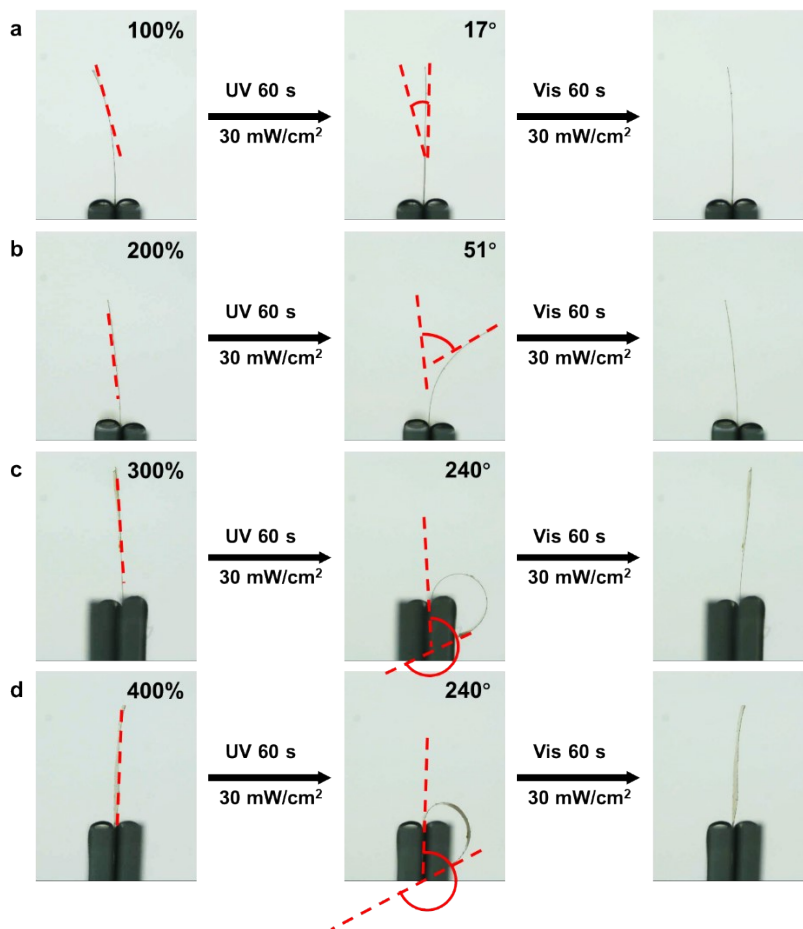


Fig. S11 Reversible photo-induced bending behavior of stretched films with different stretching ratio under UV and visible light irradiation. The bending angle corresponds to the angle between the initial form of the film and the tangent line of the bending state.

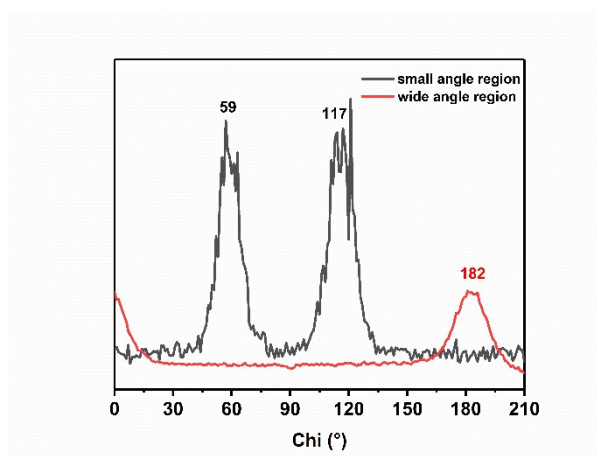


Fig. S12 Azimuthal integration of the diffraction arcs in the small/wide-angle region.

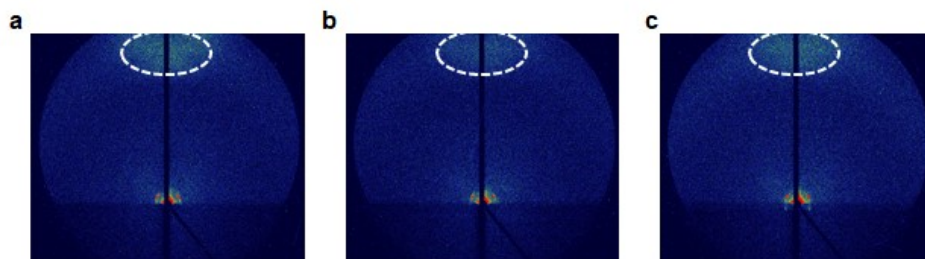


Fig. S13 Grazing incidence X-ray diffraction (GIXRD) patterns of stretched P1 film (a) before UV irradiation; (b) after UV irradiation; (c) after visible light irradiation.

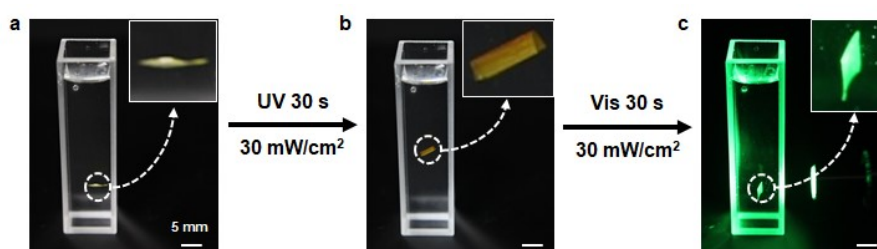


Fig. S14 Photographs to show the density change of stretched P1 film (a) before UV irradiation (365 nm, 30 mW cm⁻²); (b) after UV irradiation; (c) after visible light irradiation (530 nm, 30 mW cm⁻²).

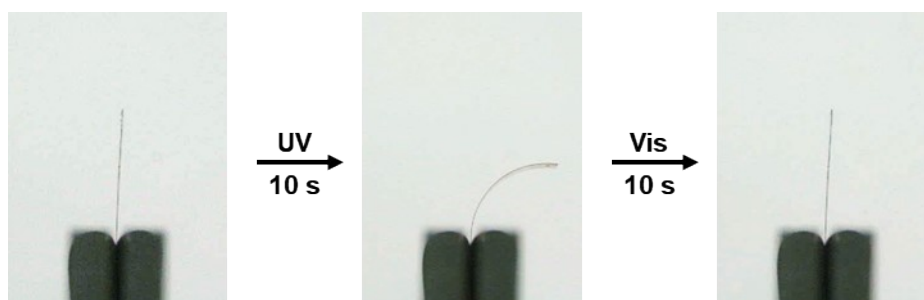


Fig. S15 Photographs to show the reversible photo-induced bending behaviors of stretched films (300%) with different stretching ratio under UV (365 nm, 30 mW cm⁻²) and visible light (530 nm, 30 mW cm⁻²) irradiation.

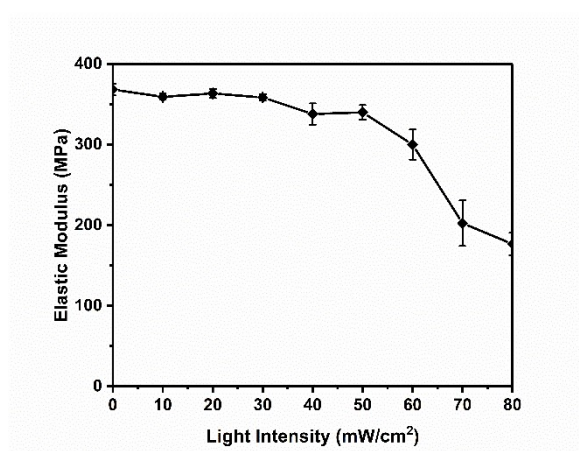


Fig. S16 Elastic modulus of the original films, and the ones after UV irradiation with different light intensity for 1 min. The sample size is: 20 mm×3 mm×20 μm.